

Theory of non-equilibrium transport in the $SU(N)$ Kondo regimeChristophe Mora¹, Pavel Vitushinsky², Xavier Leyronas³, Aashish A. Clerk², and Karyn Le Hur⁴¹Laboratoire Pierre Aigrain, ENS, Université Denis Diderot 7, CNRS; 24 rue Lhomond, 75005 Paris, France²Department of Physics, McGill University, Montreal, Quebec, Canada, H3A 2T8³Laboratoire de Physique Statistique de l'École Normale Supérieure associée au CNRS et aux Universités Paris 6 et Paris 7, 24 rue Lhomond, F-75005 Paris, France and⁴Department of Physics, Yale University, New Haven, Connecticut, USA, 06520

Using a Fermi liquid approach, we provide a comprehensive treatment of the current and current noise through a quantum dot whose low-energy behaviour corresponds to an $SU(N)$ Kondo model, focusing on the case $N = 4$ relevant to carbon nanotube dots. We show that for general N , one needs to consider the effects of higher-order Fermi liquid corrections even to describe low-voltage current and noise. We also show that the noise exhibits complex behaviour due to the interplay between coherent shot noise, and noise arising from interaction-induced scattering events. We also treat various imperfections relevant to experiments, such as the effects of asymmetric dot-lead couplings.

PACS numbers: 71.10.Ay, 71.27.+a, 72.15.Qm

I. INTRODUCTION

The Kondo effect has long served as a paradigm in the field of strongly correlated electron physics. It is perhaps the simplest example of a system where many-body interactions can give rise to highly non-trivial behavior: its essence involves nothing more than a localized magnetic impurity which is exchange coupled to conduction electrons in a metal. Despite having been studied for over 40 years, interest in Kondo physics shows no sign of abating. A large part of this continued interest has been fueled by recent advances allowing the controllable realization of unusual Kondo effects in nanostructures. These include multi-channel Kondo effects [1], where there are many conserved flavours of conduction electrons: such systems can give rise to non-Fermi liquid physics, and have recently been realized using semiconductor quantum dots [2]. Another class of exotic Kondo effects are so called $SU(N)$ Kondo effects, where $N > 2$. Such systems involve only a single channel of conduction electrons, but the effective spin of the impurity and conduction electrons is greater than $1/2$. While such systems are still described at low-energies by a Fermi liquid fixed point, the properties of this Fermi liquid are modified in several interesting ways compared to the spin- $1/2$ case [3]. The case $N = 4$ has received particular attention due to its realizability in double [4, 5, 6] and triple quantum dots [7] as well as carbon nanotube quantum dots [8, 9, 10, 11, 12].

Research on Kondo physics has also been spurred by the possibility of studying experimentally its behaviour when driven out-of-equilibrium, where non-equilibrium is either achieved by the application of a drain-source voltage across a quantum dot [13, 14], or by externally radiating a quantum dot [15]. The non-equilibrium induced by a voltage has been the subject of a number of recent theoretical works [16, 17, 18, 19, 20, 21, 22].

In this paper, we will focus on a topic which combines two of the above avenues of Kondo research: we will study non-equilibrium charge transport through a

voltage-biased quantum dot exhibiting an $SU(N)$ Kondo effect, focusing on the low-temperature regime where the physics is described by an effective Fermi liquid theory. We present calculations for both the non-linear conductance as well as for the current noise. As has been stressed in a number of recent papers [23, 24, 25], the fluctuations of current through a Kondo quantum dot are extremely sensitive to the two-particle interactions associated with the underlying Fermi liquid theory. This was first discussed in the case of the standard $SU(2)$ Kondo effect by Sela et al. [23], and was even measured for this system in a recent experiment by Zarchin et al. [26]. As discussed in Refs. [24, 25], the situation becomes even more interesting for $N > 2$, as now one must deal with the interplay between coherent partition noise (due to the zero-energy transmission coefficient through the dot not being one) and the interaction-induced scattering events. Of particular interest is the case $N = 4$, which can be realized in carbon nanotube quantum dots. Very recently, current noise in such a system has been measured experimentally by Delattre et al. [27], though not in the low-temperature Fermi liquid regime we describe here.

The results presented here both clarify and extend those presented in Refs. [24, 25], as well as provide details underlying the calculational approach. Particular attention is given to the role of higher-order Fermi liquid corrections, something that was not correctly treated in previous works (see erratum, Ref. [28]). We show clearly how in the $N = 4$ case, such corrections lead to an effective shift of the Kondo resonance with applied bias voltage. As a result, the non-linear conductance does not increase with voltage, as would be expected from a simple picture of the Kondo resonance as a resonant level sitting above the Fermi energy. These Fermi-liquid energy shifts are absent in the usual $N = 2$ Kondo effect. We also describe the experimentally-relevant case where there is an asymmetry in the coupling between the quantum dot and the source and drain electrodes. Such an asymmetry has not been investigated thoroughly in previous works.

The remainder of this paper is structured as follows. In Sec. II, we outline the basic description of our model and the Fermi liquid approach. Sec. III and IV are devoted to providing a detailed discussion of our results for both the conductance and the shot noise, as well as details on their derivation. In Sec. V, we summarize our main results for the conductance and shot noise of a $SU(N)$ Kondo quantum dot, and conclude.

II. MODEL DESCRIPTION

A. Kondo Hamiltonian

We give here a compact synopsis of the quantum dot model we study, and how it gives rise to Kondo physics. The dot connected to the leads is described by the following Anderson Hamiltonian [29]

$$H = H_D + H_L + H_T = \sum_k \epsilon_k n_k + U \sum_{n=0}^N n(n-1) + \sum_{k; \uparrow} t_L (c_{L,k}^\dagger c_{L,k} + c_{R,k}^\dagger c_{R,k}) + \sum_{k; \downarrow} (t_L c_{L,k}^\dagger + t_R c_{R,k}^\dagger) d + \text{h.c.} \quad (1)$$

$c_{L=R,k}$ is the annihilation operator for an electron of spin $\sigma = 1:::N$ and energy $\epsilon_k = \epsilon_F + k$ (measured from the Fermi energy ϵ_F) connected on the left/right lead. d is the electron operator of the dot and $n = d^\dagger d$ the corresponding density. U denotes the charging energy, ϵ_d the single particle energy on the dot and $t_{L=R}$ the tunneling matrix elements from the dot to the left/right lead. The general case of asymmetric leads contacts is parameterized by $t_L = t \cos \theta$, $t_R = t \sin \theta$ with $\theta = [0; \pi/2]$. $\theta = \pi/4$ recovers the symmetric case. The rotation in the basis of lead electrons

$$\begin{pmatrix} b_k \\ a_k \end{pmatrix} = \begin{pmatrix} \cos \theta & \sin \theta \\ \sin \theta & \cos \theta \end{pmatrix} \begin{pmatrix} c_{L,k} \\ c_{R,k} \end{pmatrix}; \quad (2)$$

decouples the a_k operators from the dot variables. The Kondo screening then involves only the b_k variables. In the symmetric case, $\theta = \pi/4$, b_k and a_k represent respectively even and odd wavefunctions with the dot placed at $x = 0$.

We consider in this work the Kondo limit where the charging energy U is by far the largest energy scale. Below this energy, the charge degree of freedom on the dot is quenched to an integer value and does not fluctuate. For $\mu_d = U(1 - m - m/N)$, the number of electrons is $n = m$. The virtual occupation of other charge states by exchange tunneling with the leads is accounted for by the standard Schrieffer-Wolff transformation [30] (or second order perturbation theory). It transforms Eq. (1) to the Kondo Hamiltonian

$$H = \sum_k \epsilon_k (b_k^\dagger b_k + a_k^\dagger a_k) + H_K \quad \text{where} \quad H_K = J_K \sum_{k, k'; \sigma} d^\dagger d_\sigma \frac{m}{N} b_{k'0}^\dagger b_{k0} \quad (3)$$

and $J_K = \frac{t^2}{U} \frac{N^2}{m(N-m)}$. This Hamiltonian acts in the subspace constrained by $n = m$. In this paper, we concentrate on the choice $\mu_d = U(1 - m - m/N)$ for which potential scattering terms vanish after the Schrieffer-Wolff transformation. Including potential scattering in the formalism is possible, for example along the line of Ref. [31]. It however remains outside the scope of this work where we focus on the asymmetric dot-lead couplings.

The lead electrons transform under the fundamental representation of $SU(N)$. With exactly m electrons, the localized spin on the dot transforms as a representation of $SU(N)$ corresponding to a single column Young tableau of m boxes. A basis of generators for this $SU(N)$ representation is formed by the $N^2 - 1$ traceless components $S^A_\sigma = d^\dagger d_\sigma (m - N)$; σ with $(\sigma, 0) \in (N; N)$. This basis can be used [32] to rewrite Eq. (3) as an antiferromagnetic coupling

$$H_K = J_K \mathbf{S} \cdot \mathbf{T}; \quad (4)$$

between the impurity (dot) spin $\mathbf{S} = (S^A; A = 1:::N^2 - 1)$ and the spin operator of the lead electrons taken at $x = 0$, $\mathbf{T} = (t_{k,k'; \sigma}; b_{k0}^\dagger t^A_\sigma, b_{k0}^\dagger; A = 1:::N^2 - 1)$. The $N - N/m$ matrices t^A are generators of the fundamental representation of $SU(N)$, while S^A are $\frac{N!}{m!(N-m)!} \frac{N!}{m!(N-m)!}$ matrices acting on states with m electrons.

Starting from high energies, J_K grows under renormalization. It presages the complete screening of the dot spin by the formation of a many-body $SU(N)$ singlet in the ground state. A large body of studies has shown that the strong coupling fixed point that dominates at low energy is a Fermi liquid one. Exact results from the Bethe-Ansatz [33] and low energy exponents that characterize a Fermi liquid. Writing the Kondo Hamiltonian (3) in terms of current, Aek [34] has shown by completing the square that the impurity spin can be absorbed by lead electrons. The resulting (conformal field) theory is that of free fermions and it is believed to describe the strong coupling fixed point. It shows a simple translation of energies in the spectrum corresponding to an electron phase shift imposed by the Friedel sum rule

$$\phi_0 = \frac{m}{N} \pi; \quad (5)$$

The identification of the leading irrelevant operator at this fixed point yields Fermi liquid behavior [31]. Alternatively and following Ref. [1] the ground state of Eq. (4) has been shown [32] to be a singlet state. Turning the coupling to the leads does not destabilize this singlet leading again to Fermi liquid exponents. Finally, Numerical Renormalization Group (NRG) calculations have confirmed this picture for $SU(2)$ [35] and $SU(4)$ [4, 5, 8, 10].

B. Fermi liquid theory

We now discuss in detail the Fermi liquid theory for the Kondo effect, first introduced by Nozières [36]. It describes the low energy regime – the vicinity of the strong coupling fixed point – and allows one to make quantitative predictions even in an out-of-equilibrium situation. In Ref. [3], the Fermi liquid theory of Nozières has been extended with the introduction of the next-to-leading order corrections to the strong coupling fixed point. These corrections are necessary in the $SU(N)$ case for observables like the current and the noise since their energy ($k_B T$, eV or $\mu_B B$) dependence is mostly quadratic.

The Kondo many-body singlet (also called the Kondo cloud) having been formed, we wish to describe how lead electrons scatter on it. At low energies, two channels open: an elastic and an inelastic one. Both take place at the dot position $x = 0$. Elastic scattering is described by an energy-dependent phase shift. At the Fermi level μ_F , it is equal to ϕ_0 , see Eq. (5). We expand the phase shift around the Fermi energy,

$$\phi_{el}(\mu) = \phi_0 + \frac{1}{T_K} \mu + \frac{2}{T_K^2} \mu^2; \quad (6)$$

where the energy μ is measured from μ_F . ϕ_0 and ϕ_2 are dimensionless coefficients of order one.

It is instructive to think of the elastic scattering on the Kondo singlet in terms of an effective non-interacting resonant level model (RLM), where this effective resonance represents the many-body Kondo resonance. This is the picture of the Kondo effect provided by slave-boson mean-field theory [37], and is an exact description of the $SU(N)$ Kondo effect in the large N limit [38]. Note that for finite N , one must also deal with true two-particle scattering on the singlet, something that will never be captured by the RLM; we thus only use it to obtain insight into the elastic scattering properties. In the RLM picture, the first two terms in the phase shift in Eq. (6) are attributed to a Lorentzian scattering resonance centered at $\mu_K = T_K \cot \phi_0$ with a width Γ/T_K [25]. In the $SU(4)$ case, one thus finds that the Kondo resonance is centered at a distance $\mu_K = T_K$ above the Fermi energy, giving a heuristic explanation for the fact that the low-energy transmission coefficient through the dot is only $T = 1/2$. The fact that the Kondo resonance sits above the Fermi energy is indeed seen in exact NRG calculations of the impurity spectral density [8, 10].

The low energy expansion of the RLM phase shift $\phi(\mu) = \arctan \frac{\mu}{\mu_K}$ also gives the form Eq. (6) with $\phi_2 = \frac{2}{T_K} = \cot \phi_0$. Note that there is no a priori reason that this relation must hold for the expansion of the true phase shift, as the correspondence to a non-interacting resonant level is not exact. Despite this caveat, one finds that the prediction from the RLM picture is quite good even at a quantitative level. The exact relation between ϕ_1 and ϕ_2 is extracted [3] from the Bethe ansatz solution [33] and

reads

$$\frac{\phi_2}{\phi_1} = \frac{N}{N-1} \frac{2}{1} \frac{(1-N) \tan(\phi_0/2)}{1 + \frac{1}{N}} \cot \phi_0; \quad (7)$$

where ϕ_0 is given Eq. (5). In the $SU(2)$ case, or more generally for a half-filled dot with $m = N/2$, $\phi_2 = 0$, corresponding to a Kondo resonance centered at the Fermi level. This is expected for a model where particle-hole symmetry is not broken. In the $SU(4)$ case, Eq. (7) gives $\phi_2 = \frac{2}{1} \cdot 1.11284$ instead of 1 in the RLM. As expected, the agreement becomes even better at larger N , and RLM result is indeed the $N \rightarrow \infty$ limit of Eq. (7).

The phase shift in Eq. (6) completely characterizes the low-energy elastic scattering on the Kondo singlet. For further calculations, it is useful to describe it using a Hamiltonian formulation. The free Hamiltonian describing purely elastic scattering is given by

$$H_0 = \sum_{\mathbf{k}} \left(b_{\mathbf{k}}^\dagger b_{\mathbf{k}} + a_{\mathbf{k}}^\dagger a_{\mathbf{k}} \right); \quad (8)$$

Decoupled from the outset, the $a_{\mathbf{k}}$ variables are the same as in the original model. In contrast, the $b_{\mathbf{k}}$ variables have been modified to now include the elastic phase shift $\phi(\mu)$ in Eq. (6). This point will be expanded on in Sec. III when we discuss the calculation of the current.

We turn now to inelastic effects, which arise from quasiparticle interactions in the Fermi liquid theory. These interactions can be written in a Hamiltonian form [3]

$$\begin{aligned} H_{int} = & \frac{1}{2T_K} \sum_{\langle \mathbf{k}, \mathbf{f}; \mathbf{k}_1, \mathbf{g} \rangle} : b_{\mathbf{k}_1}^\dagger b_{\mathbf{k}} b_{\mathbf{f}}^\dagger b_{\mathbf{g}} : \\ & + \frac{2}{4} \frac{1}{2T_K^2} \sum_{\langle \mathbf{k}, \mathbf{f}; \mathbf{k}_1, \mathbf{g} \rangle} \sum_i (b_{\mathbf{k}_1}^\dagger) : b_{\mathbf{k}_1}^\dagger b_{\mathbf{k}_2} b_{\mathbf{f}}^\dagger b_{\mathbf{g}} b_{\mathbf{k}_3}^\dagger b_{\mathbf{k}_4} : \\ & - \frac{2}{3T_K^2} \sum_{\langle \mathbf{k}, \mathbf{f}; \mathbf{k}_1, \mathbf{g} \rangle} \sum_{\langle \mathbf{k}_2, \mathbf{f}; \mathbf{k}_3, \mathbf{g} \rangle} : b_{\mathbf{k}_1}^\dagger b_{\mathbf{k}_2} b_{\mathbf{f}}^\dagger b_{\mathbf{g}} b_{\mathbf{k}_3}^\dagger b_{\mathbf{k}_4}^\dagger b_{\mathbf{k}_5}^\dagger b_{\mathbf{k}_6} : \end{aligned} \quad (9)$$

where $::$ denotes normal ordering and $\rho = 1/(h v_F)$ is the density of state for 1D fermions moving along one direction. To summarize, the Fermi liquid theory is generated by the Hamiltonian $H = H_0 + H_{int}$, given by Eqs. (8) and (9), with the elastic phase shift (6). In fact, Eqs. (6) and (9) correspond to a systematic expansion of the energy [3, 36], compatible with the $SU(N)$ symmetry and the Pauli principle. It includes all first and second order terms in the low energy coupling strength Γ/T_K .

The great advantage of the Fermi liquid approach is that it can also be applied to non-equilibrium situations. Note that the Fermi level μ_F appears twice in the above equations: it defines the reference for energies in the elastic phase shift (6) and also for the normal ordering in Eq. (9). When the system is put out-of-equilibrium, for instance when each lead has its own Fermi level, μ_F loses

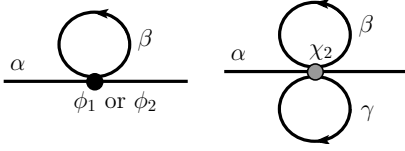


FIG. 1: Examples of Hartree diagrams for the self-energy built from Eq. (9). The full dots (resp. black and grey) indicate vertices with four or six external lines. α , β , and γ denote spins.

its meaning as a Fermi level and becomes merely an absolute energy reference. This can be used to relate [3] the coefficients (χ_1 ; χ_2 ; χ_1 ; χ_2 ; χ_2) as we shall show below.

C. Kondo coating and perturbation theory

To make progress in calculating physical observables at low energies, we will treat the interacting part H_{int} (c.f. Eq. (9)) of the Fermi-liquid Hamiltonian perturbatively. Among the various diagrams built from Eq. (9), it is convenient to separate the trivial Hartree contributions to the electron self-energy from the more complicated diagrams. The former are obtained by keeping an incoming and an outgoing line and by closing all other external lines to form loops as shown Fig. 1. The resulting diagrams are then in correspondence with the diagrams describing scattering by a local potential. Therefore they can be included in the elastic phase shift,

$$\begin{aligned} \chi'' &= \chi_0 + \frac{1}{T_K} \chi'' + \frac{2}{T_K^2} n^2 \sum_{\alpha\beta} \frac{1}{T_K} N_{0;\alpha} + \frac{2}{2T_K^2} \\ &\quad \sum_{\alpha\beta} \chi''_{\alpha\beta} \chi''_{\alpha\beta} \\ \chi''(N_{0;\alpha} + E_{1;\alpha}) &= \frac{2}{T_K^2} \sum_{\alpha\beta} \chi''_{\alpha\beta} N_{0;\alpha} N_{0;\beta} ; \end{aligned} \quad (10)$$

where we have defined $N_{0;\alpha} = \sum_k d'' n''(k)$ and $E_{1;\alpha} = d'' n''(k)$. $n''(k) = n''(k) - (n''_F)$ is the actual quasiparticle distribution ($n''(k) = \hbar \delta_k - b_k$) relative to the ground state with Fermi energy ϵ_F . We see again that ϵ_F sets the reference in Eq. (10) for both χ'' and $n''(k)$. Including Hartree diagrams is essentially tantamount to a mean-field treatment of the interaction term Eq. (9). On a physical level, these Hartree terms can be interpreted as a mean-field energy shift of the Kondo resonance arising from a finite quasiparticle population and their interactions. We shall see that in the case of an $SU(4)$ Kondo quantum dot, these Hartree terms play a significant role in determining the non-linear conductance; this is not the case in the more conventional $SU(2)$ Kondo effect.

While the idea of perturbatively treating H_{int} is straightforward enough, a possible weakness of the Fermi liquid approach is the number of seemingly undetermined

parameters in Eqs. (6) and (9). The standard Fermi liquid treatment of the Kondo effect allows one to relate the coefficients χ_1 and χ_2 via the so-called 'coating' of the Kondo resonance (to be discussed below); these coefficients correspond to leading-order Fermi liquid corrections. However, for transport quantities in the general $SU(N)$ Kondo case, we will see that the remaining coefficients, corresponding to higher-order corrections, are also important. Luckily, these too can be related to one another using a novel and powerful extension of the Kondo coating recently proposed in Ref. [3]. It allows to relate the different phenomenological coefficients of Eqs. (6) and (9); we describe the basic reasoning involved in what follows.

The Kondo resonance is a many-body phenomenon that results from the sharpness of the Fermi sea boundary [39]. Physically, conduction electrons build their own resonance. The structure of this resonance is therefore changing with the conduction electron occupation numbers, as Eq. (10) shows explicitly. However it can not depend on ϵ_F , which is a fixed energy reference. This idea is implemented by shifting the Fermi level ϵ_F by ϵ_F while keeping the absolute energy $\epsilon_F + \epsilon$ and the absolute occupation numbers $n''(k)$ fixed in Eq. (10). As a result $n''(k) \rightarrow n''(k) + (n''_F - n''_F)$. Imposing invariance of the phase shift leads to the following Fermi liquid identities

$$\chi_1 = (N - 1) \chi_1; \quad (11a)$$

$$\chi_2 = \frac{N}{4} \chi_2; \quad \chi_2 = (N - 2) \chi_2; \quad (11b)$$

where the first relation (11a) was initially derived for the general $SU(N)$ case by Nozières and Blandin [1].

Note that an alternative way to derive Eqs. (11) is to insist that the entire structure of the Kondo resonance simply translates in energy when we dope the system with quasiparticles in a way that corresponds to a simple increase of the Fermi energy [3]. Nozières' original derivation of Eq. (11a) in the $SU(2)$ case [36] also used this idea, but restricted attention to an initial state with no quasiparticles. Eqs. (11b) follow when we apply the same reasoning to an initial state having some finite number of quasiparticles. Note that for $SU(2)$, or a half-filled dot ($m = N/2$), $\chi_2 = 0$ from Eq. (7) so that $\chi_2 = 0$ and $\chi_2 = 0$. The next-to-leading order corrections all vanish in agreement with previous works on the ordinary $SU(2)$ case [23, 36, 40, 41].

It is worth mentioning that the second generation of Fermi liquid terms (χ_2 ; χ_2 ; χ_2) can also be derived in the framework of conformal field theory. In Ref. [3], a single cubic Casimir operator is given, which reproduces the three terms corresponding to the coefficients χ_2 ; χ_2 , and χ_2 . The identities (11b) are then automatically satisfied.

The coating of the Kondo resonance (and resulting conditions) also has an important consequence for calculations of observables in the presence of a voltage: the results will not depend on where one decided to place the

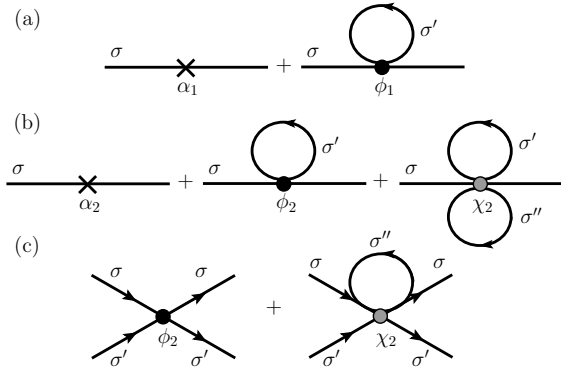


FIG. 2: Diagrammatic construction for the independence of observables in μ_F . Crosses correspond to elastic scattering. Two- and three-particle interactions are represented by, respectively, black and grey full circles. Many diagrams in the perturbative expansion in H_{int} (9) exhibit a dependence in μ_F . Nevertheless, it is possible to gather and combine those diagrams to produce μ_F -invariant forms. The combination (a) that appears in the irreducible selfenergy does not depend on μ_F as a result of Eq. (11a). Combination (b) is a second invariant, thanks to Eqs. (11b), contributing to the irreducible selfenergy. (a) and (b) together imply the phase shift invariance discussed in the text. Finally, the four-particle vertices of (c) can always be combined to cancel the dependence in μ_F thanks to Eq. (11b). Apart from (a), (b) and (c), all other diagrammatic parts involve energy differences in which the reference μ_F naturally disappears. The combinations (a), (b) and (c) can be understood as emerging from Ward identities related to the $U(1)$ gauge symmetry. For example, Eq. (11a) has been shown [42, 43] to derive from a Ward identity with a vanishing charge susceptibility.

dot Fermi energy μ_F within the energy window defined by the chemical potentials of the leads. On a technical level, this is because, by virtue of Eqs. (11), any shift μ_F of the dot Fermi energy will be completely compensated by a corresponding shift in the Hartree contributions arising from the quasiparticle interactions. This invariance is explained in detail in Fig. 2. Note also that this invariance has physical consequences as well: it implies, for example, that the current is not affected by the capacitive coupling to the leads (in the Kondo limit).

Given the above invariance, it is convenient for calculations to choose the Fermi level such that

$$\sum_{\mathbf{Z}} N_{0,\mathbf{Z}} = \sum_{\mathbf{Z}} d \mathbf{n}(\mathbf{Z}) = 0; \quad (12)$$

so that any closed fermionic loop built from an energy-independent vertex vanishes. For this choice of position, $N_{0,\mathbf{Z}}$ vanishes which greatly simplifies the phase shift expression (10). Moreover, the χ_2 vertex in Eq. (9) does not contribute to the current and the noise when the perturbative calculation is stopped at second order. The reason for that is that the χ_2 vertex is already second order and can only appear once. Its six legs are connected to at most two current vertices so that at least two of these legs must connect to form a closed loop implying

a vanishing contribution. In contrast to these simplifications, E_1 in Eq. (10) remains generally different from zero due to the energy dependence of the χ_2 vertex in Eq. (9).

One may wonder whether the physical argument of the coating of the Kondo resonance, as presented in Ref. [3] and repeated in this paper, is sufficient to extend the results of this paper to higher orders Fermi liquid corrections. Applying the coating argument to the next (third) order, one obtains an incomplete set of relations between the coefficients such that some of them remain undetermined. In the language of conformal field theory, it means that more than one operator is involved at each (higher) order. How to relate the coefficients of those operators is a rather difficult problem. In the $SU(2)$ case, a solution was given by Lesage and Saleur [44].

We now turn to the discussion of the Fermi liquid model renormalization. Treated naively, the model leads to divergences in physical quantities. It is regularized [31] by introducing an energy cutoff D (different from the original band width of the model) larger than typical energies of the problem but smaller than T_K . Energies in Eq. (8) are therefore restricted to the window $[-D; D]$. The dependence of observables in D is then removed by adding counterterms in the Hamiltonian. It is strictly equivalent to the introduction of cutoff D dependence in the coupling constants [45] (\tilde{t}_i, \tilde{t}_i , etc). The corresponding counterterms are discussed in Appendix A.

III. CURRENT CALCULATION

We now outline the calculation of the current using the Fermi liquid theory described in previous sections. Again, the complete Hamiltonian is $H = H_0 + H_{\text{int}}$ (c.f. Eqs. (8,9)), corresponding to respectively to elastic and inelastic scattering; the approach will be to treat H_{int} as a perturbation. Slightly abusing terminology, we will include all Hartree contributions arising in perturbation theory in the free Hamiltonian H_0 ; H_0 will thus correspond to the elastic phase shift given in Eq. (10). Contributions to the current which only involve H_0 (thus defined) will be referred to as the 'elastic current'. H_{int} is then added perturbatively, without Hartree diagrams, in order to compute the corrections due to inelastic scattering.

A. The current operator

The current operator at x is generally given by

$$\hat{I}(x) = \frac{e\hbar}{2m} \sum_{\mathbf{Z}} \mathbf{v}(\mathbf{Z}) \partial_x \psi(\mathbf{Z}) \psi(\mathbf{Z}) + \text{c.c.} \quad (13)$$

where m is the electron mass. Various expressions can be obtained for the current depending on which basis it is expanded. It is convenient [24] in our case to choose the

basis of scattering states that includes completely elastic (and Hartree terms) scattering, i.e. the phase shift (10), and that correspond to eigenstates of the single-particle scattering matrix. Such states will have waves incident from both the left and right leads. This is in contrast to another standard choice [25], which is to use scattering states which either have an incident wave from the left lead, or from the right. We refer to such states as the 'left/right' states.

We first discuss our scattering states in first quantization. Eigenfunctions corresponding to the a_k variables do not see the dot or the Kondo effect. Using Eq. (2), they read

$$a_{k\sigma}(x) = \begin{cases} \sin(e^{i(k_F + k)x}) & x < 0; \\ \cos(e^{i(k_F + k)x}) & x > 0; \end{cases} \quad (14)$$

where $\phi = 4m$ measures the asymmetry of the coupling to the leads, see Eq. (2), and the eigenenergies $\epsilon_k = \epsilon_F + k$ are measured from the Fermi level ϵ_F . The situation is more complicated for the b_k variables. The associated eigenfunctions at small x , close to the dot, depend on the complex ground state wavefunction of the Kondo problem. They are not known, and in fact it can not even be reduced to a one-particle problem. However, we can write the eigenfunctions far from the dot,

$$b_{k\sigma}(x) = \begin{cases} \cos(e^{i(k_F + k)x}) & x < 0; \\ \sin(e^{i(k_F + k)x}) & x > 0; \end{cases} \quad (15)$$

where the S matrix is related to the phase shift (10), $S_k = e^{2i\phi(k)}$ at eigenenergy $\epsilon_k = \epsilon_F + k$. The eigenstates (14) and (15) have the same energy. They can be combined to give the left and right scattering states with the energy-dependent transmission $T(\epsilon) = \sin^2(2\phi)\sin^2(\phi)$. In the $SU(2)$ case (or generally particle-hole symmetric case), $\phi_0 = \pi/2$ and the system is closed to unitarity for symmetric leads coupling.

We come back to second quantization and project the electron operator $\psi(x)$ over the eigenstates (14) and (15). Conservation of the current implies that $\hat{I}(x)$ does not depend on x . We choose an arbitrary $x < 0$ far from the dot, \hat{I}_L is the current at x and \hat{I}_R at $-x$. If \hat{I} denotes the conserved current, $\hat{I} = \hat{I}_L = \hat{I}_R$. The combination $\sin^2\phi \hat{I}_L + \cos^2\phi \hat{I}_R$ leads to the compact expression

$$\hat{I} = \frac{e}{2h} \sum_k \sin 2\phi [a^\dagger(x)b(x) - a^\dagger(-x)b(-x) + \text{h.c.}] + 2\cos 2\phi [a^\dagger(x)a(x) - a^\dagger(-x)a(-x)]; \quad (16)$$

with $b(x) = \sum_k b_k e^{ikx}$ and $Sb(x) = \sum_k S_k b_k e^{ikx}$. Physically, operators taken at $x(-x)$ correspond to incoming (outgoing) states [46]. The second line in Eq. (16) turns out not to contribute to the mean current, the noise or any moment of the current.

Before proceeding with the calculation, it is worth noting that in the $SU(2)$ case, the proximity to the unitary situation allows a simpler treatment [47]. The current is written $\hat{I} = I_L - I_R$ with $I_\alpha = \frac{2e^2}{h} V$. All quantum or thermal fluctuations are included in the backscattering current \hat{I}_{BS} which can be written in terms of a_k and b_k operators [41, 48]. However, the range of application of this approach is restricted to the $SU(2)$ case with a completely symmetric leads coupling. In any other situations neglecting fluctuations in I_L is incorrect [24, 25] and Eq. (16) becomes necessary.

B. Elastic contribution to the current

We are now in a position to compute the mean value of the current in an out-of-equilibrium situation. A dc bias is applied between the two electrodes imposing $\epsilon_L - \epsilon_R = eV$. Left and right scattering states, corresponding to $c_{L,k}$ and $c_{R,k}$ operators, are in thermal equilibrium with chemical potentials ϵ_L and ϵ_R . Hence, using Eq. (2), we obtain the populations

$$\langle b_{k\sigma}^\dagger b_{k\sigma} \rangle = \langle c_{k\sigma}^\dagger c_{k\sigma} \rangle \cos^2\phi_L(\epsilon_k) + \sin^2\phi_R(\epsilon_k); \quad (17a)$$

$$\langle a_{k\sigma}^\dagger a_{k\sigma} \rangle = \langle c_{k\sigma}^\dagger c_{k\sigma} \rangle \sin^2\phi_L(\epsilon_k) + \cos^2\phi_R(\epsilon_k); \quad (17b)$$

$$\langle a_{k\sigma}^\dagger b_{k\sigma} \rangle = \langle b_{k\sigma}^\dagger a_{k\sigma} \rangle = \frac{k_{F0} \sin 2\phi}{2} [\phi_L(\epsilon_k) - \phi_R(\epsilon_k)]; \quad (17c)$$

$$\phi_{L=R}(\epsilon) = \phi(\epsilon_{L=R}); \quad (17d)$$

for all spins σ . Eq. (12), that implies a vanishing Hartree diagram, is satisfied with $\phi_L = \sin^2\phi eV$ and $\phi_R = \cos^2\phi eV$. $f(\epsilon) = (1 + e^{\beta(\epsilon - \epsilon_F)})^{-1}$ is the Fermi distribution.

The average current is obtained from Eq. (16) and reproduces the Landauer-Büttiker formula [46]

$$I_{el} = \frac{Ne}{h} \sum_k \frac{d}{d\epsilon} T(\epsilon) [\phi_L(\epsilon) - \phi_R(\epsilon)]; \quad (18)$$

with the transmission

$$T(\epsilon) = \sin^2 2\phi \sin^2(\phi(\epsilon)); \quad (19)$$

and the phase shift

$$\phi(\epsilon) = \phi_0 + \frac{1}{T_K} \epsilon + \frac{2}{T_K^2} \epsilon^2 - \frac{(\phi'(\epsilon))^2}{3} - \frac{(eV)^2 \sin^2 2\phi}{4}; \quad (20)$$

where we have used the identity (11b), $\phi_2 = (\phi_1 - 1)\phi_2 = 4$. Here, the phase shift $\phi(\epsilon)$ has an extra (V/T) dependence due to mean-field (Hartree) interaction contributions (cf. Eq. (10)). Within the heuristic resonant-level picture, we can interpret this as the voltage inducing a quasiparticle population, whose interactions in turn yield a mean-field upward energy shift of the Kondo resonance. Note that the relevant interactions here are not the leading-order Fermi liquid interactions described by ϕ_1 , but rather the next-leading-order interaction described by ϕ_2 .

At zero temperature, the current can be expanded to second order in $eV = T_K$. The asymmetry and the zero-energy transmission are characterized by

$$C = \cos 2\theta; \quad T_0 = \sin^2 \theta \quad (21)$$

with $C = 0$ in the symmetric case. The current takes the form

$$\begin{aligned} \frac{I_{e1}}{(1 - C^2)N e^2 V = \hbar} &= T_0 - C \sin 2\theta - \frac{eV}{2T_K} \\ &+ \frac{eV}{T_K} \cos 2\theta (1 + 3C^2) \frac{1}{12} - \sin 2\theta (1 - 3C^2) \frac{1}{6} : \end{aligned} \quad (22)$$

C. Inelastic contribution to the current

The Keldysh framework [49] is well-suited to estimate interaction corrections (9) to the current. The mean current takes the form

$$I = \hbar T_c \hat{I}(t) e^{-\frac{1}{\hbar} \int_C dt^0 H_{\text{int}}(t^0)} i; \quad (23)$$

where the Keldysh contour C runs along the forward time direction on the branch $= +$ followed by a backward evolution on the branch $= -$. T_c is the corresponding time ordering operator. Time evolution of $\hat{I}(t)$ and $H_{\text{int}}(t)$ is in the interaction representation with the unperturbed Hamiltonian H_0 (8). Mean values $\langle \dots \rangle$ are also taken with respect to H_0 (8) with bias voltage, see Eqs. (17). Note that the time t in Eq. (23) is arbitrary for our steady-state situation. Finally, in order to maintain the original order of operators in $\hat{I}(t)$, we take left (creation) operators on the $= -$ branch and right (annihilation) one on the $= +$ branch.

A perturbative study of Eq. (23) is possible by expansion in H_{int} and use of Wick's theorem. This leads to usual diagrammatics where one should keep track of the Keldysh branch index. The lowest order recovers the results of Sec. IIIB describing elastic scattering. The next first order gives only Hartree terms already included in Eq. (22). H_{int} gives rise in general to three vertices with coefficients γ_1 , γ_2 and γ_3 where the last two are already second order in $1 = T_K$. Thus it is consistent to keep only γ_1 in the second order expansion in H_{int} . A typical Green's function is defined by $G_{ab}^{1;2}(x, x^0; t, t^0) = i\hbar T_c a(x; t; \gamma_1) b^\dagger(x^0; t^0; \gamma_2) i$. For clarity, spin indices are omitted here and below since all noninteracting Green's functions are spin diagonal. Noninteracting Green's functions are 2×2 matrices in

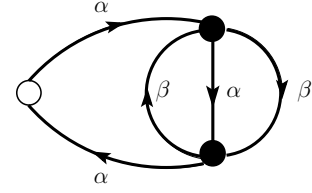


FIG. 3: Second order diagram describing the interaction correction to the current from Hamiltonian Eq. (9). The open circle represents a current vertex while filled black dots correspond to interaction vertices. α, β are spin degrees of freedom. The self-energy term is formed by the three lines connecting the two interaction vertices.

Keldysh space given in momentum-energy space by

$$G_{bb}(k; \omega) = \frac{1}{\omega - \epsilon_k} z + i \frac{F_0}{F_0 - 1} \frac{F_0 + 1}{F_0} (\omega - \epsilon_k) \quad (24a)$$

$$G_{aa}(k; \omega) = \frac{1}{\omega - \epsilon_k} z + i \frac{F_0}{F_0 - 1} \frac{F_0 + 1}{F_0} (\omega - \epsilon_k) \quad (24b)$$

$$G_{ab}(k; \omega) = G_{ba}(k; \omega) = 2i \hbar a_k^\dagger b_k i \frac{1}{1} \frac{1}{1} (\omega - \epsilon_k); \quad (24c)$$

with the Pauli matrix $\sigma_z = \begin{pmatrix} 1 & 0 \\ 0 & -1 \end{pmatrix}$, $F_0(\omega_k) = 2\hbar a_k^\dagger b_k i$, and $F_0'(\omega_k) = 2\hbar a_k^\dagger a_k i - 1$, as given Eqs. (17). We wish to compute the second order correction from Eq. (23). It involves the self-energy contribution shown in Fig. 3 and defined by

$$\begin{aligned} G_{bb}^{1;2}(t_1, t_2) &= \sum_{k_1, k_2, k_3} G_{bb}^{1;2}(k_1; t_1, t_2) \\ &G_{bb}^{2;1}(k_2; t_2, t_1) G_{bb}^{1;2}(k_3; t_1, t_2) \end{aligned} \quad (25)$$

The causality identity, for $t \neq 0$,

$$G_{bb}^{++}(t) + G_{bb}^{--}(t) = G_{bb}^{+-}(t) + G_{bb}^{-+}(t); \quad (26)$$

is derived by writing the explicit time dependence in Eq. (25). It leads to various cancellations, in particular for terms where the lines external to the self-energy (25) bear no $\omega_{1=2}$ dependence. The lines that join the current vertex to the self-energy in Fig. 3 travel from x (or $-x$) to 0 (the dot) and the opposite. Thus, using the Green's function (24a) in real space (with $\omega = 1$)

$$G_{bb}^{1;2}(x, x; \omega) = i \int dx' e^{i\omega x' - \epsilon x'} F_0(\omega) + \frac{1}{2} = 1 \quad (27)$$

and the identity (26), one shows that the terms with operators taken at x in Eq. (16) give a vanishing contribution to the current. This is merely a consequence of

causality: interaction, which takes place at $x = 0$, can only affect outgoing current and not the incoming part. We are left with the current correction

$$I_{\text{int}} = \frac{N(N-1)e\sin 2}{2h} \frac{1}{2T_K} \sum_{\sigma} \int_{-\infty}^{\infty} d\epsilon \left(iS G_{bb}^{+; \sigma}(\epsilon; \sigma) - iS G_{ba}^{+; \sigma}(\epsilon; \sigma) + \text{c.c.} \right) \quad (28)$$

The summation over σ_1 and σ_2 gives two terms: (i) one includes the combination $\sigma_1 = \sigma_2$. It gives a contribution proportional to D exactly cancelled by a counterterm. Details are given in Appendix A. (ii) the second term involves the combination $\sigma_1 = -\sigma_2$ and remains finite in the limit $D \rightarrow \infty$. It reads

$$I_{\text{int}} = \frac{N(N-1)(1-C^2)e}{2h} \frac{1}{2T_K} \sum_{\sigma} \int_{-\infty}^{\infty} d\epsilon \left(f_L(\epsilon) - f_R(\epsilon) \right) \quad (29)$$

with C given by Eq. (21) and $f_L(\epsilon) = f_L(\epsilon) - f_R(\epsilon)$.

We proceed further and restrict ourselves to the zero-temperature case. The left and right Fermi step functions are introduced by going to frequency space for Eq. (25), and then by using Eqs. (24a) and (17). The result involves a sum of terms with products of \cos^2 and \sin^2 . Two distinct integrals,

$$J_1 = \int_{-\infty}^{\infty} d\epsilon \int_{-\infty}^{\infty} d\epsilon' f_L(\epsilon) f_L(\epsilon') \quad (30a)$$

$$J_2 = \int_{-\infty}^{\infty} d\epsilon \int_{-\infty}^{\infty} d\epsilon' f_L(\epsilon) f_R(\epsilon') \quad (30b)$$

corresponding respectively to one- and two-particles transfer, appear with the following combination

$$\cos^2 \sin^2 (J_2 - 2J_1) + J_1 = \frac{J_2(1-C^2) + 2J_1(1+C^2)}{4} \quad (31)$$

With $J_1 = (eV)^3/6$ and $J_2 = 4(eV)^3/3$, we obtain the current correction

$$\frac{I_{\text{int}}}{(1-C^2)N e^2 V/h} = \cos 2\theta_0 (N-1) \frac{1}{T_K} \frac{eV}{h} \frac{5}{12} \frac{C^2}{4} \quad (32)$$

This result can be given a quite simple physical interpretation along the line of Ref. [23]. The I_1 term in the interaction part of the Hamiltonian (9) can be decomposed on the left/right operators basis using Eq. (2). It then describes processes where 0, 1 or 2 electrons are transferred from one scattering state to the other. Using Fermi's golden rule and $\cos^6 \sin^2 + \cos^2 \sin^6 = (1-C^4)/8$, the total rate of one-electron transfer is evaluated to be $2\sigma_1(1-C^4)$ where

$$\sigma_1 = N(N-1) \frac{eV}{h} \frac{1}{24} \frac{eV}{T_K} \quad (33)$$

From $\cos^4 \sin^4 = (1-C^2)^2/16$, the total rate for two-electron transfer is $2\sigma_2(1-C^2)^2/2$ where $\sigma_2 = 8\sigma_1$. For one- and two-electron transfers, $e\cos 2\theta_0$ and $2e\cos \theta_0$ are interpreted as the corresponding charge transferred between leads [25]. Writing the current correction as

$$I_{\text{int}} = (e\cos 2\theta_0)2\sigma_1(1-C^4) + (2e\cos \theta_0)\frac{2}{2}\sigma_2(1-C^2)^2;$$

we recover Eq. (32).

D. Current for SU(2) and SU(4)

The results of Secs. IIIB, IIIC can be extended to finite temperature as explained in Appendix B. We detail results for the total current $I = I_{\text{el}} + I_{\text{int}}$ in the $(N=2; m=1)$ case and $(N=4; m=1; 2)$ cases.

For SU(2), a single electron is trapped on the dot, $\sigma_1 = 1$ and $\sigma_2 = 0$. The current takes the form

$$I = I_m \left(1 - \frac{1}{T_K} \frac{(eV)^2}{2} + (T)^2 \right) \quad (34)$$

where $I_m = (2e^2 V/h)(1-C^2)$. In the particle-hole SU(4) symmetric case with two electrons, $\sigma_1 = 3$ and $\sigma_2 = 0$. The current reads

$$I = I_m \left(1 - \frac{1}{T_K} \frac{2(eV)^2}{9} + \frac{C^2(eV)^2}{6} + \frac{5(T)^2}{9} \right) \quad (35)$$

where $I_m = (4e^2 V/h)(1-C^2)$.

Turning now to the SU(4) case with one electron on the dot, one finds that the inelastic contribution to the current vanishes identically (c.f. Eq. (32)), as the effective charges associated with interaction-induced scattering events are proportional to $\cos 2\theta_0$ and hence identically zero [25]. The only contribution is thus from the elastic channel (c.f. Eq. (22)), yielding:

$$I = I_m \left(1 - \frac{1}{T_K} \frac{C eV}{3} - \frac{2}{T_K} \frac{eV}{3} (1-3C^2) \right) \quad (36)$$

where $I_m = (2e^2 V/h)(1-C^2)$. There is no temperature correction up to this order of the low energy expansion. The case with three electrons ($m=3$) and SU(4) symmetry is related to the one-electron case by particle-hole symmetry. The Kondo resonance is thus changed from above to below the Fermi energy. The result for the current is then the same as Eq. (36), but with an opposite sign for the asymmetry ($\theta_0 \rightarrow \pi - \theta_0$, $C \rightarrow -C$), i.e. the roles of left (L) and right (R) leads are exchanged for hole transport.

The differential conductance $G(V) = \frac{dI}{dV}(V)$ obtained from Eq. (36) gives an asymmetric curve whenever $C \neq 0$. Consider the first the strongly asymmetric case, where \mathcal{J} becomes sizeable. In this case, the asymmetric linear $eV = T_K$ correction in Eq. (36) dominates even at low

bias voltage. For strong asymmetry $j \ll 1$, the conductance measures the density of states of the Kondo resonance [50] at eV . The asymmetric linear term thus follows the side of the Kondo resonance and reveals that the resonance peak is located away from the Fermi level [12]. This behaviour is in fact generic to the $SU(N)$ case when the occupation of the dot is away from half-filling. In the $SU(2)$ case or generally for a half-filled dot ($m = N/2$), the resonance peak is located at the Fermi level which suppresses the asymmetric linear term, see Eqs. (34) and (35).

Turning now to the case of a symmetric dot-lead coupling ($C = 0$), we see that as expected, the differential conductance $G(V)$ is symmetric in V at all dot fillings; hence, it exhibits a quadratic behaviour at low bias. In the $SU(4)$ case, the conductance obtained from Eq. (36) is predicted to be maximum at $V = 0$, in agreement with results obtained from slave boson mean field theory [27]. Within the Fermi liquid approach, and for one electron on the dot, this behaviour is at first glance rather puzzling. As we have already indicated, in the $SU(4)$ case, the conductance is completely due to the elastic transport channel. Using the heuristic picture provided by the resonant level picture (i.e. elastic scattering due to a Lorentzian Kondo resonance sitting above the Fermi energy), one would expect that the differential conductance should increase with increasing voltage, due to the positive curvature of the expected (Lorentzian) transmission coefficient. This picture is in fact incorrect, as it neglects the important Hartree contributions discussed in Sec. IIIB. Heuristically, as the voltage is increased, quasiparticle interactions lead to a mean-field upward energy shift of the position of the Kondo resonance. Because of the relation $\gamma = (4/3)\gamma_0$, this energy-shift effect dominates, and causes the conductance to decrease; without this mean-field energy shift, the conductance would indeed exhibit a quadratic increase at small voltages. Note that an incorrect upturn in the conductance was reported in previous works: Ref. [25] neglected the higher-order Fermi liquid interaction parameter γ and the resulting mean-field energy shift, while Ref. [24] treated it incorrectly (corrected in [28]). Note also that the results for the conductance presented in Ref. [12] only apply to a system with a strongly asymmetric dot-lead coupling.

IV. CURRENT NOISE

Fluctuations in the current are almost as important as the current itself. In particular, the shot noise (at zero temperature) carries information about charge transfer in the mesoscopic system. The purpose of this section is to detail the calculation of the zero-frequency current noise,

$$S = \frac{2}{\tau} \int_0^\tau dt \langle \hat{I}(t) \hat{I}(0) \rangle; \quad (37)$$

with the current fluctuation $\hat{I}(t) = \hat{I}(t) - \langle \hat{I}(t) \rangle$, see Eq. (16) for the current operator expression.

Insight can be gained by first examining the strong coupling fixed point at zero temperature, with $eV \ll T_K$ so that $\langle \hat{I} \rangle = 0$. Quantum expectations in Eq. (37) are evaluated with the free Hamiltonian (8). The shot noise,

$$S_0 = \frac{2N e^3 \gamma}{h} T_0 (1 - C^2) [1 - T_0 (1 - C^2)]; \quad (38)$$

is pure partition noise like a coherent scatterer [46]. This result implies a vanishing noise in the particle-hole symmetric case, like standard $SU(2)$, with symmetric leads coupling ($T_0 = 1$ and $C = 0$). In this specific case, the shot noise is only determined by the vicinity of the Kondo strong coupling fixed point, that is by the inelastic Hamiltonian (9) and the corrections to γ_0 in the elastic phase shift (6). The shot noise is therefore highly non-linear with $S \propto V^3$ at low bias voltage. Since the corresponding current is close to unitarity, an effective charge $e^* = (5/3)e$ has been extracted from the ratio of the noise to the backscattering current [23]. $e^* \neq e$ should however not be confused with a fractional charge. It emerges as an average charge during additional and independent Poissonian processes involving one and two charges transfer as shown by the calculation of the full counting statistics [48]. Nevertheless, this charge $e^* = (5/3)e$ is universal and characterizes the vicinity of the Kondo strong coupling fixed point. It can be seen as an out-of-equilibrium equivalent of the Wilson ratio.

In asymmetric situations ($T_0 \neq 1$ or $C \neq 0$), the linear part (38) of the noise does not vanish and even dominates at low bias voltage. For instance in the $SU(4)$ case, $T_0 = 1/2$ so that $T_0(1 - T_0) = 1/4$. This property is quite relevant for experiments and may be used to discriminate $SU(2)$ and $SU(4)$ symmetries for which the current gives essentially the same answer [27]. In a way similar to the symmetric $SU(2)$ case, we can define an effective charge from the ratio of the non-linear parts ($\propto V^3$) in the noise and the current [24, 25]. This is however less straightforward to measure experimentally since it requires a proper subtraction of the linear terms.

A. Elastic contribution to the noise

Inserting the current operator (16) in Eq. (37), the elastic Hamiltonian (8) gives a gaussian measure which allows to use Wick's theorem, and thus Eqs. (17). Like for the current, we obtain a Landauer-Buttiker formula [46] for the noise with the same transmission (19) and phase shift (20). At zero temperature, it reads

$$S = \frac{2N e^2}{h} \sum_{\alpha} \int_0^\tau dt \langle \hat{I}^2(t) \rangle [1 - T(\alpha)]; \quad (39)$$

An expansion to second order in $eV = T_K$ yields the elastic (non-linear) correction to the noise (38),

$$\frac{S_{e1}}{(1 - C^2)2N e^3 \hbar \nu} = \frac{S_{e1}^{(1)} eV}{T_K} + \frac{S_{e1}^{(2)} eV^2}{T_K^2}; \quad (40)$$

with coefficients,

$$S_{e1}^{(1)} = \frac{C}{2} \frac{1 - \sin^2 \theta_0}{2} [1 - 2T_0 (1 - C^2)]; \quad (41a)$$

$$S_{e1}^{(2)} = \frac{1}{12} (1 + 3C^2) (\cos 4\theta_0 + 2 \sin \theta_0 \sin 3\theta_0 C^2) \\ - \frac{2}{6} (1 - 3C^2) \sin 2\theta_0 [1 - 2T_0 (1 - C^2)]; \quad (41b)$$

and the total elastic noise reads $S_{e1} = S_0 + S_{e1}$. The first order correction (41a) gives an asymmetric part to the noise for $C \neq 0$. In a way similar to the current case, particle-hole transformation ($\theta_0 \rightarrow \pi - \theta_0$, $\nu \rightarrow -\nu$) reverts the sign of the asymmetry (41a) which indicates that the Kondo resonance is centered on the Fermi level.

B. Inelastic contribution to the noise

We follow the same procedure as for the interaction correction to the current established in Sec. III C. The mean value in Eq. (37) is taken within the Keldysh framework, similar to Eq. (23). The correct ordering of \hat{I} operators is maintained by choosing time 0 on the $\rightarrow +$ branch and time t on the $\rightarrow -$ branch. The perturbative study of the noise involves diagrams with two current vertices instead of one in Sec. III C. The resulting calculations are therefore similar to those for the current but are much more involved on the technical side. The diagrams relevant for the noise at first and second order in $1/T_K$ are shown in Fig. 4. Noninteracting Green's functions are still given by Eqs. (24).

Three vertices can be built from the interaction Hamiltonian H_{int} (9) with coefficients γ_1 , γ_2 and γ_3 . The γ_2 vertex has six legs and appears at most once at order $1/T_K^2$. Topology therefore imposes that two legs among the six must connect to form a closed loop. The corresponding energy integral vanishes thanks to Eq. (12). Apart from Hartree terms already included in the elastic part, see Sec. IV A, the expansion to first order in H_{int} gives the single diagram 4a. Involving both γ_1 and γ_2 , the interaction vertex in diagram 4a is characterized by the energy dependent coefficient $\langle \sigma_i \sigma_j \rangle = \gamma_1 + \gamma_2 (\sigma_i + \sigma_j) = 2T_K$. The corresponding noise correction is given by

$$S_{int}^a = \frac{i e^2 (1 - C^2) N (N - 1)}{4 \nu^2 \hbar T_K} \times \int \frac{d\omega d\omega_0}{(2\pi)^2} A(\omega) \langle \sigma_i \sigma_j \rangle A(\omega_0); \quad (42)$$

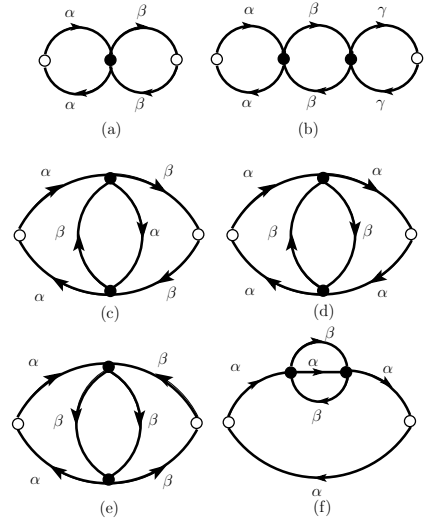


FIG. 4: Diagrams for the noise appearing in the first and second order expansions in the inelastic Hamiltonian Eq. (9). Diagrams (c) and (d) give identical contributions. For diagram (f), the three-lines bubble can alternatively dress the bottom Green's function. \uparrow, \downarrow denote spins with $\pm 1/2$ and \uparrow, \downarrow . Open dots represent current vertices while filled black dots correspond to interaction vertices.

where $A^{1/2}$ is the building block defined in Appendix C and shown in Fig. 6. We replace $A^{1/2}$ by its expression (C 9) (with $\sin^2(\theta)$ instead of T_0) and perform the summation to get

$$\frac{S_{int}^a}{(1 - C^2)^2 2N e^3 \hbar \nu} = \frac{(N - 1)}{T_K} \int d\omega d\omega_0 f(\omega) f_0(\omega) \sin^2(\theta(\omega)) \langle \sigma_i \sigma_j \rangle \sin 2\theta(\omega_0); \quad (43)$$

This general expression can finally be expanded order by order in $eV = T_K$. After energy integration, we obtain at zero temperature a first and a second order noise term,

$$\frac{S_{int}^a}{(1 - C^2)^2 2N e^3 \hbar \nu} = \frac{S_{int}^{(a;1)} eV}{T_K} + \frac{S_{int}^{(a;2)} eV^2}{T_K^2}; \quad (44)$$

with coefficients,

$$S_{int}^{(a;1)} = C \frac{1}{2} (N - 1) \sin 2\theta_0 \sin^2 \theta_0; \quad (45a)$$

$$S_{int}^{(a;2)} = C^2 \frac{1}{2} (N - 1) [2T_0 \sin 2\theta_0 + 6 \frac{1}{2} T_0 (1 - 4T_0/3)]/2; \quad (45b)$$

Note that these two terms vanish identically for symmetric leads coupling ($C = 0$). It can be checked again that the first order correction is odd with respect to particle-hole symmetry while the second order is even.

The expansion to second order in H_{int} yields the diagrams 4b-f with two interaction vertices. To be consistent with the rest of the perturbative calculation, only γ_1 is kept in each interaction vertex. The contributions

corresponding to the diagrams 4b-f are all calculated in Appendix C. Finally, the total noise reads

$$S = S_0 + S_{e1} + S_{int}^a + S_{int}^b + 2 S_{int}^c + S_{int}^e + S_{int}^f; \quad (46)$$

where the different terms are respectively given by Eqs. (38), (40), (44), (C 19), (C 12), (C 16) and (C 6).

C. Noise for SU (2) and SU (4)

We have also extended the noise calculation to finite temperature along the lines of Appendix B. In the asymmetric case, the results are too cumbersome to be written here. In the symmetric case, the noise was calculated in Ref. [24] where it was emphasized that corrections are rapidly sizeable at finite temperature. Hence the shot noise regime is expected only at very low temperature. Keeping a zero temperature, we specialize here to the experimentally relevant SU (2) and SU (4) cases with one electron on the dot, $m = 1$.

In the SU (2) case, the noise correction to Eq. (38) reads

$$\frac{S}{(1 - C^2) 2N e^3 j \hbar} = \frac{eV}{T_K} \left[\frac{2}{1} - \frac{5}{6} - \frac{4}{3} C^2 \right]; \quad (47)$$

where the C^4 terms cancel each other unexpectedly.

In the SU (4) case, the noise correction has linear and quadratic contributions,

$$\begin{aligned} \frac{S}{(1 - C^2) 2N e^3 j \hbar} &= \frac{eV}{T_K} \left[\frac{C}{2} (1 - 2C^2) \right. \\ &+ \left. \frac{eV}{T_K} \left[\frac{2}{18} (1 - 8C^2 + 7C^4) - \frac{2}{6} (1 - 3C^2) \right] \right]; \end{aligned} \quad (48)$$

V. RESULTS AND CONCLUSION

A. Main Results

Following Refs [24, 25], we define a generalized Fano factor F which describes the relation between the non-linear current and current noise:

$$F = \frac{1}{2e} \frac{S}{I}; \quad (49)$$

It is defined as the ratio between the non-linear parts of the noise $S = S_{NL}$ (c.f. Eq. (38)) and of the current $I = I_{NL}$, where

$$I_0 = (1 - C^2) \frac{N T_0 e^2 V}{h}; \quad (50)$$

is the linear current (for $eV = T_K$). We focus on the non-linear noise and current, as it is these quantities which are sensitive to the contribution of Fermi liquid interactions.

Consider first the strong asymmetric case $j \neq 1$ (i.e. $\phi \neq 0$ or $\phi = 2$), where the dot is strongly coupled

to one lead and only weakly to the other (c.f. Eq. (2)). Transport in this limit corresponds to an incoherent tunneling regime where the hopping from the weakly-coupled lead to the dot is the limiting process. It can be checked from the Eqs. (40), (44), (C 19), (C 12), (C 16), (C 6) for the noise, and Eqs. (22), (32) for the current, that the Fano factor $F = 1$ to leading order in $1/j$. This is of course expected since the tunneling regime gives Poissonian statistics for charge transfer. Note that this unity ratio holds order by order for the $eV = T_K$ and $(eV = T_K)^2$ correction separately. In addition, we also have $S_0 = 2eI_0 = 1$ to leading order in $1/j$.

In the opposite limit of a symmetric dot-lead coupling (i.e. $C = 0$), coherent effects are important to transport, and charge transport is generally not Poissonian [48]. Note also that in the symmetric case, the non-linear parts of both the current and current noise are $\propto V^3$. We find that the generalized Fano factor (49) is given by

$$F = \frac{1 + \sin^2(2\phi_0) + \frac{9}{N} \frac{13 \sin^2(2\phi_0)}{1} - \frac{2}{1} \sin 4\phi_0}{\frac{N+4}{N-1} \cos 2\phi_0 - \frac{2}{1} \sin 2\phi_0}; \quad (51)$$

This Fano factor includes the effect of interactions; we have used the important equalities in Eqs. (11). Note that this result has no explicit dependence on $V = T_K$: it is thus a universal quantity characterizing the Fermi liquid properties of the strong-coupling fixed point; also note that F is invariant under a particle-hole transformation, where $m \rightarrow N - m$. We stress that the fact $F \neq 1$ in general is due both to the existence of two-particle scattering at the fixed point, as well as to the partition noise associated with single-particle scattering. We give in Table I values of F for different N and m .

For $N \rightarrow 1$, Eq. (51) leads to

$$F = \frac{3 \cos 4\phi_0 + 4 \cos 2\phi_0}{4 + 2 \cos 2\phi_0}; \quad (52)$$

Note that in the large N limit, two-particle scattering processes become insignificant [51] for the current (since ϕ_1 and ϕ_2 scale as $1/N$) and the result is consistent with the non-interacting resonant level. In this limit, the Wilson ratio is in fact just one [1, 38]. However, the effect of two-particle scattering processes seems to survive in the current noise through the diagram of Fig. 4(b). Heuristically, this diagram represents an enhancement of the coherent partition noise already present in the absence of Fermi liquid interactions. The small interaction parameter $\frac{2}{1} \frac{1}{N^2}$ is compensated by the spin summation with N^3 equivalent diagrams. The effect is therefore linear in N , at the same level as elastic term s .

The expression of Eq. (52) can be checked in two limiting cases. For $\phi_0 \rightarrow 0$, it gives $F \rightarrow 1$. Again it corresponds to the tunneling regime since a small phase shift ϕ_0 implies a weak electronic transmission $T_0 = \sin^2 \phi_0$. When particle-hole symmetry is recovered, $\phi_0 = \pi/2$, we find $F = 1$. In this limit, the conductance is close to unitarity and interactions play no role since the diagram

m	N							
	2	3	4	5	6	7	8	9
1	-5/3	-0.672	-0.300	-0.156	0.003	0.156	0.287	0.393
2		-0.672	-3/2	-1.256	-1.031	-0.855	-0.679	-0.503
3			-0.300	-1.256	-7/5	-1.326	-1.254	-1.173
4				-0.156	-1.031	-1.326	-4/3	-1.313

TABLE I: Fano factor F , Eq. 49, for various N and m .

of Fig. 4 (b) gives a vanishing contribution for $\phi_0 = \pi/2$. The situation is therefore similar to the ordinary SU (2) case [23, 48] where one has Poissonian weak backscattering events. In our case though, backscattering events are elastic and imply the transfer of only one electron so that $F = 1$.

We now turn to the general asymmetric case, $C \neq 0$, where we focus on the SU (2) and SU (4) symmetries with $m = 1$. For SU (2), the generalized Fano factor

$$F = \frac{5}{3} + \frac{8}{3} C^2; \quad (53)$$

is obtained from the ratio of the noise (47) and current (34) corrections at zero temperature. We stress that this simple result (53) is exact and is not restricted to small values of the asymmetry C . Eq. (53) indeed bridges the symmetric result $F = 5/3$ [23] to the tunneling regime, $F = 1$ in the strong asymmetry limit $C \rightarrow 1$. A different asymmetry correction was predicted in Ref. [23]. This discrepancy may come from the fact that the current expression used in Ref. [23] is not valid outside the symmetric case $C = 0$ (see discussion at the end of Sec. III A).

The SU (4) case for arbitrary asymmetry is more complicated since the generalized Fano factor (49) bears a $eV = T_K$ dependence. This is because the non-linear current and noise have both linear and quadratic corrections in $eV = T_K$ (resp. quadratic and cubic terms in V) and no simplification occurs when the ratio is computed (universality is however recovered in the symmetric case where the linear corrections vanish). We therefore prefer to compute directly the ratio of the quadratic corrections with the result

$$F^{(2)} = \frac{1}{2e} \frac{S^{(2)}}{I^{(2)}} = \frac{\frac{2}{3}}{\frac{1}{2}} \frac{1}{1} \frac{8C^2 + 7C^4}{3C^2} + C^2; \quad (54)$$

where $S^{(2)}$ ($I^{(2)}$) denotes the noise (current) correction to second order in $eV = T_K$. Again the ratio (54) connects the symmetric case ($N = 4, m = 1$ in Table I), $F^{(2)} = \frac{5}{3}$, [23] to the tunnel or strongly asymmetric regime where $F^{(2)} = 1$. Expanding Eq. (54) in C , we obtain $F^{(2)} = \frac{5}{3} (1 - 8/3 C^2)$ which indicates an important correction due to the asymmetry of the coupling to the leads.

B. Conclusion

To summarize, we have provided a thorough analysis of the non-equilibrium transport in the SU (N) Kondo

regime using an elaborate Fermi-liquid approach.

We have particularly focused on the case $N = 4$ relevant to carbon nanotube quantum dots. One important characteristic of the emergent SU (4) symmetry is the sign change of the leading current corrections (i.e. linear in $eV = T_K$) as a function of the bias voltage when progressively tuning the asymmetry between the dot-lead couplings. More precisely, for a strong asymmetry, we have recovered a positive linear correction which traduces the fact that the Kondo resonance is peaked away from the Fermi level; in this case, the conductance measures the density of states of the Kondo resonance at eV where the sign changes with the weakly coupled lead. For symmetric couplings, we have demonstrated that the linear correction now becomes exactly zero and that the current becomes maximum at $V = 0$ due to interactions via the Hartree contributions. In addition, the noise exhibits a non-trivial form due to the interplay between coherent shot-noise and noise arising from interaction-induced scattering events. In the symmetric case, interactions result in a universal Fano factor $F = 5/3$ at zero temperature. For a finite asymmetry between dot-lead couplings, the current and the noise have both linear and quadratic corrections in $eV = T_K$. Focusing exclusively on the quadratic corrections, we have derived a formula for the Fano factor which extrapolates between the symmetric result and the strongly asymmetric result $F = 1$, perfectly reproducing the Poissonian statistics for charge transfer in the tunneling limit.

In the context of the standard SU (2) Kondo effect, we have obtained a generalized Fano factor $F = 5/3 + 8C^2/3$ at zero temperature which is not restricted to small values of the asymmetry. Finally, in the limit of large N , it is certainly relevant to observe that the effect of interactions tends to subsist in the current noise.

Acknowledgments: The authors are grateful to M.-S. Choi, T. Kontos, and N. Regnault for interesting discussions. A.C. thanks NSERC, CIFAR and the McGill Centre for the Physics of Materials for support. K.L.H. acknowledges the support from the Department of Energy in USA under the grant DE-FG 02-08ER 46541 and is grateful to ENS Paris for the kind hospitality.

APPENDIX A: COUNTERTERMS AND MODEL RENORMALIZATION

The improper self-energy can be calculated to second order in $\Gamma = T_K$ following Refs. [12, 31]. The result is that

the dependence on the cutoff D can be removed by adding the counterterm

$$H_{c;1} = \frac{1}{2} \frac{1}{T_K} \sum_{\mathbf{k}, \mathbf{k}^0}^X \left(\mathbf{b}_{\mathbf{k}}^{\dagger} + \mathbf{b}_{\mathbf{k}^0}^{\dagger} \right) : \mathbf{b}_{\mathbf{k}}^{\dagger} \mathbf{b}_{\mathbf{k}^0} : \quad (\text{A } 1)$$

$$1 = \frac{1}{2} \frac{1}{T_K} \frac{6D}{4} \ln \frac{4}{3}$$

to the Hamiltonian $H_0 + H_{\text{int}}$, Eqs. (8), (9). It corresponds to a renormalization of $1 \rightarrow 1 + 1$.

We will now show that the second contribution that arises from Eq. (28), and that we have discarded in Sec. IIIC, produces a term linear in D exactly cancelled by the counterterm (A 1). Using the identity $\text{sgn}(t) = \text{sgn}(t) (\text{sgn}(t) + 1)$, it takes the form

$$I_{\text{int}}^{(2)} = N(N-1) \frac{e}{2h} \frac{1}{2T_K} \int_{-D}^D dt \text{sgn}(t) \left(\text{sgn}(t) + 1 \right) \left(\mathbf{f}(t) \cdot \mathbf{f}(t) + c.c. \right) \quad (\text{A } 2)$$

where $\mathbf{f}(t)$ is the time Fourier transform of $\mathbf{f}(\omega) = \mathbf{f}_L(\omega) - \mathbf{f}_R(\omega)$. Inserting the Fourier transform of $F_0 = 1$,

$$\frac{1}{D} \frac{d}{dt} \left(F_0(\omega) - 1 \right) e^{i\omega t} = \frac{T}{\sinh(Tt)} \quad (\text{A } 3)$$

$$(2 \cos^2 e^{iLt} + 2 \sin^2 e^{iRt}) \frac{2e^{-iD} t}{t}$$

in Eq. (25) with Eq. (24a), it can be checked that intermediate values of $t = T; 1=V$ give a vanishing result for Eq. (A 2) (integrand is odd in t). Eq. (A 2) is therefore dominated by small $t = D$. In that limit, $\text{sgn}(t) \rightarrow \text{sgn}(t) = \text{sgn}(t)$ and $\text{sgn}(t) = \text{sgn}(t)$.

$\mathbf{f}(t) = \mathbf{f}(0) + t \mathbf{f}'(0)$ is expanded to first order in t since the zeroth order gives an odd integrand and a vanishing integral. After some straightforward algebraic manipulations, we eventually find the result

$$\frac{I_{\text{int}}^{(2)}}{(1 - C^2)N e h} = \frac{1}{\sin 2\theta} \frac{d}{dt} \left(\frac{1}{T_K} [\mathbf{f}_L(\omega) - \mathbf{f}_R(\omega)] \right); \quad (\text{A } 4)$$

where we have used that

$$\int_0^{\infty} (du u^2) (1 - e^{-iu})^3 = 3 \ln(3/4):$$

When higher orders in t are included in the expansion, corrections to Eq. (A 4) are of order $O(1=D)$ and completely vanish in the universal limit $D \rightarrow \infty$. In particular, the $O(1)$ contribution vanishes by symmetry. Finally, the counterterm (A 1) gives an elastic contribution to the current that can be computed along the lines of Sec. IIIB. The result compensates exactly Eq. (A 4).

A second counterterm is generated by vertex corrections. In the spirit of the self-energy calculation, the singular contributions (i.e. depending on the cutoff D) to

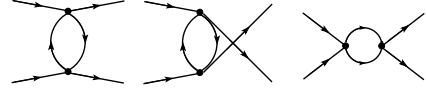


FIG. 5: $\frac{2}{1}$ corrections to the four-particle vertex.

the four-particle vertex are determined from the standard second order diagrams shown in Fig. 5, and proportional to $\frac{2}{1}$. This strong dependence on D is removed by the counterterm

$$H_{c;2} = \frac{1}{2T_K} \sum_{\mathbf{k}_1, \mathbf{k}_2, \mathbf{k}_3, \mathbf{k}_4}^X : \mathbf{b}_{\mathbf{k}_1}^{\dagger} \mathbf{b}_{\mathbf{k}_2}^{\dagger} \mathbf{b}_{\mathbf{k}_3}^{\dagger} \mathbf{b}_{\mathbf{k}_4}^{\dagger} : \quad (\text{A } 5)$$

$$1 = (N-2) \frac{2}{1} \frac{D}{T_K} \frac{4}{4} \ln 2:$$

To summarize, the perturbative calculation of observables to second order in $\omega = T_K$ (ω is a typical energy, $\omega_B, k_B T$ or eV), from the full Hamiltonian $H_0 + H_{\text{int}} + H_{c;1} + H_{c;2}$, leads to finite and well-defined results in the universal limit $D \rightarrow \infty$.

APPENDIX B: FINITE TEMPERATURE CURRENT

We briefly outline how the current is calculated at finite temperature. For the elastic part (18) detailed in Sec. IIIB, we merely need the Fourier transform of $\mathbf{f}(\omega) = \mathbf{f}_L(\omega) - \mathbf{f}_R(\omega)$,

$$\mathbf{f}(t) = e^{iLt} - e^{iRt} \frac{1}{2} \frac{T}{\sinh(Tt)}; \quad (\text{B } 1)$$

The derivatives of $\mathbf{f}(t)$, taken at $t = 0$, give access to the integrals with the corresponding powers of ω in Eq. (18).

The inelastic part of the current is detailed in Sec. IIIC and given by Eq. (29). Eq. (29) is evaluated at finite temperature by Fourier transform to real time t . The time contour is then shifted by i in the complex plane, with $D = 1$ (but $T, eV = 1$) such as to suppress the dependence on the cutoff D in Green's functions. From Eq. (A 3), the result is (for $x = 0$)

$$G_{bb}^+(t) = (\cos^2 e^{iLt} + \sin^2 e^{iRt}) \frac{T}{\sinh(Tt)};$$

with a similar expression for $G_{bb}^-(t)$. The intermediate integral result

$$\int_{-1-i}^{1+i} dt G_{bb}^+(t) G_{bb}^-(t) G_{bb}^+(t) G_{bb}^-(t) = \frac{5}{12} \frac{C^2}{4} (eV)^2 + \frac{2(T)^2}{3}; \quad (\text{B } 2)$$

is used to derive the current interaction correction

$$\frac{I_{\text{int}}}{(1-C^2)N e^2 V \hbar} = \cos 2\theta_0 (N-1) \frac{1}{T_K} \left[\frac{5}{12} - \frac{C^2}{4} (eV)^2 + \frac{2(T)^2}{3} \right] ; \quad (\text{B } 3)$$

The t -integral in Eq. (B 2) is obtained by first expanding the numerator in powers of $e^{iL=R}$. Each term gives an integral. The standard method to evaluate such integrals is to shift the integration contour by $i=T$ in the complex plane which encloses the pole at $x=0$.

APPENDIX C: DETAILS ON THE INTERACTION CORRECTION TO THE NOISE

We discuss in this Appendix the interaction corrections to the noise with two interaction vertices, i.e. the diagrams 4b-f. Terms $\propto 1/T_K^2$ in the interaction Hamiltonian (9) are already second order in $1/T_K$. Therefore only the term $\propto 1/T_K$ is kept for the diagrams 4b-f since the whole calculation goes up to second order in $1/T_K$.

In order to simplify the forthcoming expressions, let us define the following prefactor

$$S_P = \frac{\hbar N (N-1) \sin^2 2\theta_0}{2 \hbar} \frac{e^2}{2 \hbar} \frac{1}{T_K^2} ; \quad (\text{C } 1)$$

We start by considering the diagram 4f where the self-energy bubble is inserted in the top Green's function. Going to energy space and integrating over time t in Eq. (37), the corresponding contribution takes the form

$$S_{\text{int}}^{f,1} = S_P \sum_{1,2} \int \frac{d''}{2} \gamma^{1,2}(\omega'') P^{1,2}(\omega''); \quad (\text{C } 2)$$

where $\gamma^{1,2}(\omega'')$ is the selfenergy part (25) that already appeared in the calculation of the current. $P^{1,2}$ is a notation for the product of the three Green's functions (of the form $G^{-1} G^{2+} G^{+}$) that enclose the selfenergy in diagram 4f. Since the current operator (16) has four different terms, this gives a sum of 16 terms for $P^{1,2}$. Yet nine of these terms have no $1=2$ dependence and vanish when summed over $1=2$. This is a consequence of the causality identity (26). Finally $P^{1,2}$ reads

$$\begin{aligned} P^{1,2}(\omega'') = & (S) G_{ab}^{-1}(\omega; \omega'') G_{bb}^{2+}(\omega; \omega'') G_{ab}^{+}(\omega - 2\omega; \omega'') + (S)^2 G_{ab}^{-1}(\omega; \omega'') G_{bb}^{2+}(\omega; \omega'') G_{ab}^{+}(0; \omega'') \\ & + (S) G_{bb}^{-1}(\omega; \omega'') G_{ba}^{2+}(\omega; \omega'') G_{ba}^{+}(2\omega; \omega'') + (S)^2 G_{bb}^{-1}(\omega; \omega'') G_{ba}^{2+}(\omega; \omega'') G_{ba}^{+}(0; \omega'') \\ & + (S)(S) G_{bb}^{-1}(\omega; \omega'') G_{bb}^{2+}(\omega; \omega'') G_{aa}^{+}(0; \omega'') + (S) G_{bb}^{-1}(\omega; \omega'') G_{bb}^{2+}(\omega; \omega'') G_{aa}^{+}(\omega - 2\omega; \omega'') \\ & + (S) G_{bb}^{-1}(\omega; \omega'') G_{bb}^{2+}(\omega; \omega'') G_{aa}^{+}(2\omega; \omega'') ; \end{aligned} \quad (\text{C } 3)$$

The noise contribution with a bottom self-energy insertion gives a similar expression. Green's functions are replaced by their expression (24) and the summation over $1=2$ is performed together with the causality identity (26). In analogy with the current calculation, two sorts of terms are obtained: (i) those including the combination γ^{++} and (ii) those with γ^{+-} or γ^{-+} . Type (i) terms are dominated by energies on the order of the model cutoff D . They are exactly cancelled by the counterterm (A 1). We therefore only keep type (ii) terms. Combining top and bottom self-energy insertion diagrams, $S_{\text{int}}^f = S_{\text{int}}^{f,1} + S_{\text{int}}^{f,2}$, we find the contribution

$$\frac{S_{\text{int}}^f}{(1-C^2)2N e^3 \hbar} = \frac{i(N-1)^2}{2 \cdot 3T_K^2} \int \frac{d''}{2} [(1-C^2)(\cos 4\theta_0 - \cos 2\theta_0) [f(\omega'')]^2 + 2T_0 (F_0(\omega'') F_0(\omega'') - 1)] \times (\gamma^{+-}(\omega'') + \gamma^{-+}(\omega'')) - F_0(\omega'') - 1 + (\omega'') - F_0(\omega'') + 1 + \gamma^{++}(\omega'') \quad (\text{C } 4)$$

At zero temperature, $F_0(\omega'') F_0(\omega'') - 1 = (1+C^2) f(\omega'')$ and

$$\int_R \frac{d''}{2} \gamma^{+-}(\omega'') + \gamma^{-+}(\omega'') = i^3 \frac{5}{12} - \frac{C^2}{4} (eV)^3 ; \quad (\text{C } 5)$$

as we have shown in Sec. III C for the current. The last two terms in Eq. (C 4) involve the combination $4J_1(1+C^4) + J_2(1-C^4)$ with $J_{1=2}$ given Eqs. (30). Finally, we obtain for the noise correction (C 4),

$$\frac{S_{\text{int}}^f}{(1-C^2)2N e^3 \hbar} = (N-1)^2 \frac{eV}{T_K} \left[\frac{1}{4} - \frac{C^4}{12} + \frac{5}{24} - \frac{C^2}{8} (1-C^2)(\cos 4\theta_0 - \cos 2\theta_0) - 2T_0(1+C^2) \right] ; \quad (\text{C } 6)$$

Next we turn to the diagram 4c with the particle-hole

pair polarization bubble,

$$\gamma^{1,2}(t) = \sum_{k_1, k_2} G_{bb}^{-1,2}(k_1; t) G_{bb}^{2,1}(k_2; -t) ; \quad (\text{C } 7)$$

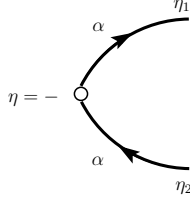


FIG. 6: Building block appearing in diagrams 4a-e defined as $A^{1;2}(\omega)$, see Eq. (C 9). It is formed by one current vertex on the branch $\omega = +$ or $\omega = -$ with two lines. The incoming line connects the branch $\omega = -$ to $\omega = +$ while the outgoing connects to $\omega = -$.

Another causality identity, similar to Eq. (26), also applies here. For $t \neq 0$,

$$G^{++}(t) + G^{--}(t) = G^{+-}(t) + G^{-+}(t): \quad (C 8)$$

An elementary building block that appears in diagrams 4a-e is shown Fig 6. It consists in one current

vertex on the branch $\omega = +$ or $\omega = -$ supplemented by one incoming and one outgoing lines. In energy space, it reads

$$A^{1;2}(\omega) = (i)^2 \sin 2\theta_f(\omega) [4T_0 F_0(\omega) + S_{11} - S_{22}]; \quad (C 9)$$

where the four terms of the current operator (16) are included. Using the definitions (C 1), (C 7), (C 9), the noise term due to diagram 4c can be written

$$S_{\text{int}}^c = S_P \sum_{1;2} \int \frac{d\omega_1}{2} \int \frac{d\omega_2}{2} A^{1;2}(\omega_1) A^{2;1}(\omega_2): \quad (C 10)$$

Following a now familiar pattern, there are terms with $\omega = +$ and others with $\omega = -$. The former ones depend linearly on the cutoff and are exactly cancelled by counterterms. This will be discussed at the end of this Appendix.

We are left with

$$\frac{S_{\text{int}}^c}{(1 - C^2)2N e^2 \hbar} = \frac{(N - 1)(1 - C^2)^2}{2^2 T_K^2} \int \frac{d\omega_1}{2} \int \frac{d\omega_2}{2} f(\omega_1) f(\omega_2) \left(\omega_1^+ \omega_2^+ + \omega_1^+ \omega_2^- \right) \cos 4\theta_0 + 2 \left(\omega_1^+ \omega_2^- + \omega_1^- \omega_2^+ \right) T_0 \cos 2\theta_0 (F_0(\omega_1) - F_0(\omega_2)): \quad (C 11)$$

At zero temperature, the second term in the brackets gives a vanishing contribution. Developing in terms of Fermi step functions, the integrals over energies can be performed leading to

$$\frac{S_{\text{int}}^c}{(1 - C^2)2N e^3 \hbar} = (N - 1) \frac{eV}{T_K} (1 - C^2) \cos 4\theta_0 \left(\frac{1}{6} - \frac{C^2}{12} \right); \quad (C 12)$$

corresponding to the combination $J_2(1 - C^2) + 4J_1 C^2$.

The diagram 4d gives exactly the same contribution, $S_{\text{int}}^d = S_{\text{int}}^c$. The calculation for the diagram 4e is quite similar with the introduction of the particle-particle bubble,

$$\tilde{A}^{1;2}(t) = \sum_{k_1, k_2} G_{bb}^{1;2}(k_1; t) G_{bb}^{1;2}(k_2; t); \quad (C 13)$$

that satisfies the same causality identity (C 8). The noise

term reads

$$S_{\text{int}}^e = S_P \sum_{1;2} \int \frac{d\omega_1}{2} \int \frac{d\omega_2}{2} A^{1;2}(\omega_1) \tilde{A}^{1;2}(\omega_1 + \omega_2) A^{1;2}(\omega_2); \quad (C 14)$$

leading to

$$\frac{S_{\text{int}}^e}{(1 - C^2)2N e^2 \hbar} = \frac{(N - 1)(1 - C^2)^2}{2^2 T_K^2} \int \frac{d\omega_1}{2} \int \frac{d\omega_2}{2} f(\omega_1) f(\omega_2) \left(\omega_1^+ \omega_2^+ + \tilde{\omega}_1^+ \omega_2^+ \right) + 2 \left(\omega_1^+ \omega_2^- + \tilde{\omega}_1^+ \omega_2^- \right) T_0 \cos 2\theta_0 (F_0(\omega_1) + F_0(\omega_2)); \quad (C 15)$$

and

$$\frac{S_{\text{int}}^e}{(1 - C^2)2N e^3 \hbar} = (N - 1) \frac{eV}{T_K} (1 - C^2) \left(\frac{1}{6} + \frac{C^2}{12} + T_0 \cos 2\theta_0 C^2 \right); \quad (C 16)$$

corresponding to the combination $J_2(1+C^2) - 4J_1C^2 + 8T_0 \cos 2\theta_0 C^2 (J_2 - 2J_1)$. We finally consider the diagram 4b that also involves the particle-hole bubble ,

$$S_{\text{int}}^b = \sum_{\mathbf{k}} (N-1) \sum_{\mathbf{k}_1, \mathbf{k}_2}^X \frac{d''_1}{2} \frac{d''_2}{2} A^{1;1}(\mathbf{k}_1) A^{2;2}(\mathbf{k}_2); \quad (\text{C } 17)$$

with the definitions (C1), (C7) and (C9). Keeping only the terms with $\mathbf{k} = 0$, we obtain

$$\frac{S_{\text{int}}^b}{(1-C^2)2N e^2 \hbar} = (1-C^2) \sin^2(2\theta_0) \frac{(N-1) f_1^2}{2T_K^2} \frac{d''}{2} f''(\mathbf{k}) (\tau_0^+ + \tau_0^-); \quad (\text{C } 18)$$

At zero temperature, $\tau_0^+ = \tau_0^- = (\hbar^2/2m^*) (1-C^2)$ so that the noise correction for diagram 4b finally reads

$$\frac{S_{\text{int}}^b}{(1-C^2)2N e^3 \hbar} = \frac{(N-1) f_1^2 \sin^2(2\theta_0)}{4} \frac{eV}{T_K} (1-C^2)^2; \quad (\text{C } 19)$$

Before concluding this long Appendix, we briefly discuss the remaining terms resulting from the τ_0^+ and τ_0^- combinations. They lead to contributions that are linear in the cutoff D , with corrections scaling as $O(1/D)$ and therefore vanishing in the universal limit. The calculation is straightforward and uses the same ingredients as in the Appendix A, i.e. small dominant time integrals. Therefore we can use $\tau_0^+(\mathbf{k}) = \tau_0^-(\mathbf{k}) = \tau_0^2(1-e^{iD\tau})^2 = \tau_0^2$, $\tau_0^+(\mathbf{k}) = \tau_0^-(\mathbf{k})$ and $\tau_0^+(\mathbf{k}) = \tau_0^-(\mathbf{k})$, $\tau_0^+(\mathbf{k}) = \tau_0^-(\mathbf{k})$ in those integrals. The final result reads

$$\frac{S_{\text{int}}^{(D)}}{(1-C^2)^2 2N e^3 \hbar} = \frac{1}{4} (N-1) C \sin 2\theta_0 \sin^2 \theta_0 \frac{eV}{T_K}; \quad (\text{C } 20)$$

where we recall that $\tau_0 = (N-2) \frac{\hbar^2 D}{4T_K} \ln 2$. This contribution is exactly cancelled by the counterterm (A5) included in the diagram of Fig. 4a.

-
- | | |
|--|---|
| <p>[1] P. Nozières, A. Blandin, J. Phys. (Paris) 41 193 (1980).
 [2] R. M. Potok, I. G. Rau, H. Shtrikman, Y. Oreg and D. Goldhaber-Gordon, Nature (London) 446 167 (2007).
 [3] C. Mora, Phys. Rev. B 80 125304 (2009).
 [4] L. Borda, G. Zarand, W. Hofstetter, B. J. Halperin, and J. von Delft, Phys. Rev. Lett 90 026602 (2003).
 [5] K. Le Hur, P. Simon, and L. Borda, Phys. Rev. B 69 045326 (2004).
 [6] R. Lopez, D. Sanchez, M. Lee, M.-S. Choi, P. Simon, K. Le Hur, Phys. Rev. B 71 115312 (2005).
 [7] T. Numata, Y. Nisikawa, A. Oguri, A. C. Hewson, arXiv:0905.3343 .
 [8] M.-S. Choi, R. Lopez, and R. Aguado, Phys. Rev. Lett 95 067204 (2005).
 [9] P. Jarillo-Herrero et al, Nature (London) 434 484 (2005).
 [10] J.S. Lim, M.-S. Choi, M.Y. Choi, R. Lopez, and R. Aguado, Phys. Rev. B 74 205119 (2006).
 [11] A. M. Akarovskii, J. Liu and G. Finkelstein, Phys. Rev. Lett 99 066801 (2007).
 [12] K. Le Hur, P. Simon, and D. Loss, Phys. Rev. B 75 035332 (2007).
 [13] S. De Franceschi et al, Phys. Rev. Lett 89 156801 (2002).
 [14] M. Grobis, I. G. Rau, R. M. Potok, H. Shtrikman, and D. Goldhaber-Gordon, Phys. Rev. Lett 100 246601 (2008).
 [15] J. M. Elzerman et al, J. Low Temp. Phys. 118 375 (2000).</p> | <p>[16] A. Rosch, J. Paaske, J. Kroha, P. Wolf, Phys. Rev. Lett 90 076804 (2003).
 [17] S. Kehrein, Phys. Rev. Lett 95 056602 (2005).
 [18] P. Mehta, N. Andrei, Phys. Rev. Lett 96 216802 (2006).
 [19] B. Doyon, Phys. Rev. Lett 99 076806 (2007).
 [20] E. Boulat, H. Saleur, and P. Schmittenekert, Phys. Rev. Lett 101 140601 (2008).
 [21] F. B. Anders, Phys. Rev. Lett 101 066804 (2008).
 [22] C.-H. Chung, K. Le Hur, M. Vojta, and P. Wolf, Phys. Rev. Lett 102 216803 (2009).
 [23] E. Sela, Y. Oreg, F. von Oppen, and J. Koch, Phys. Rev. Lett 97 086601 (2006).
 [24] C. Mora, X. Leyronas, N. Regnault, Phys. Rev. Lett 100 036604 (2008).
 [25] P. Vitushinsky, A. A. Clerk, and K. Le Hur, Phys. Rev. Lett 100 036603 (2008).
 [26] O. Zarchin, M. Zaslav, M. Heiblum, D. Mahalu, and V. Umansky, Phys. Rev. B 77 241303 (2008).
 [27] T. Delattre et al, Nature Physics 5 208 (2009).
 [28] C. Mora, X. Leyronas, N. Regnault, Phys. Rev. Lett 102 139902(E) (2009).
 [29] H. R. Krishna-murthy, J. W. Wilkins, K. G. Wilson, Phys. Rev. B 21 1003 (1980).
 [30] J.R. Schrieffer, P.A. Wolf, Phys. Rev. 149 491 (1966).
 [31] I. A. Eck and A. Wolf. Ludwig, Phys. Rev. B 48 7297 (1993).
 [32] O. Parcollet, A. Georges, G. Kotliar, A. Sengupta, Phys.</p> |
|--|---|

- Rev.B 58 3794 (1998).
- [33] V.V.Bazhanov, S.L.Lukyanov, A.M.Tsvetlik, Phys.Rev. B 68 094427 (2003).
- [34] I.Aeck, Nucl.Phys.B 336 517 (1990).
- [35] K.G.Wilson, Rev.Mod.Phys. 47 773 (1975).
- [36] P.Nozières, J.Low Temp. Phys. 17 31 (1974); P.Nozières, J.Physique 39 1117 (1978).
- [37] P.Coleman, Phys.Rev.B 29 3035 (1984).
- [38] D.M.Newns, N.Read, Adv.Phys. 36 799 (1987).
- [39] J.Kondo, Progr.Theoret.Phys. 32 37 (1964).
- [40] Y.Meir and A.Golub, Phys.Rev.Lett 88 116802 (2002).
- [41] A.Golub, Phys.Rev.B 73 233310 (2006).
- [42] A.Hewson, The Kondo Problem to Heavy Fermions (Cambridge University Press, Cambridge 1993).
- [43] A.C.Hewson, Adv.Phys. 43 543 (1994).
- [44] F.Lesage, H.Saleur, Phys.Rev.Lett 82 4540 (1999); F.Lesage, H.Saleur, Nucl.Phys.B 546 585 (1999).
- [45] C.Mora, Y.Castin, Phys.Rev.A 67 053615 (2003).
- [46] Y.M.Blanter and M.Büttiker, Phys.Rep. 366 1 (2000).
- [47] A.Kaminski, Yu.V.Nazarov, and L.I.Glazman, Phys.Rev.B 62 8154 (2000).
- [48] A.O.Gogolin and A.Komnik, Phys.Rev.Lett 97 016602 (2006).
- [49] A.Kamenev, in Nanophysics: Coherence and Transport edited by H.Bouchiat et al. (Elsevier 2005) arXiv:cond-mat/0412296.
- [50] L.I.Glazman and M.Pustilnik, in Nanophysics: Coherence and Transport edited by H.Bouchiat et al. (Elsevier 2005) pp.427-478, arXiv:cond-mat/0501007.
- [51] Z.Ratiani, A.Mitra, Phys.Rev.B 79 245111 (2009).